

Palladium nanoparticles supported on silicate-based nanohybrid material: highly active and eco-friendly catalyst for reduction of nitrobenzene at ambient conditions

Esmat Ebadati , Behzad Aghabarari , Mozhgan Bagheri , Ali Khanlarkhani & Maria Victoria Martinez Huerta

To cite this article: Esmat Ebadati , Behzad Aghabarari , Mozhgan Bagheri , Ali Khanlarkhani & Maria Victoria Martinez Huerta (2020): Palladium nanoparticles supported on silicate-based nanohybrid material: highly active and eco-friendly catalyst for reduction of nitrobenzene at ambient conditions, Inorganic and Nano-Metal Chemistry, DOI: [10.1080/24701556.2020.1799403](https://doi.org/10.1080/24701556.2020.1799403)

To link to this article: <https://doi.org/10.1080/24701556.2020.1799403>

 View supplementary material 

 Published online: 12 Aug 2020.

 Submit your article to this journal 

 Article views: 10

 View related articles 

 View Crossmark data 



Palladium nanoparticles supported on silicate-based nanohybrid material: highly active and eco-friendly catalyst for reduction of nitrobenzene at ambient conditions

Esmat Ebadati^a, Behzad Aghabarari^a, Mozhgan Bagheri^a, Ali Khanlarkhani^a, and Maria Victoria Martinez Huerta^b

^aDepartment of Nanotechnology and Advanced Materials, Materials and Energy Research Center, Tehran, Iran; ^bInstitute of Catalysts and Petrolechemistry, CSIC, Madrid, Spain

ABSTRACT

In this study, spent bleaching earth (SBE), a hazardous industrial waste was used as raw material to synthesis carbon/silicate nanohybrid material (CSNH) as support for mono and bimetallic palladium and nickel nanoparticles. The synthesized catalysts were characterized by different techniques such as nitrogen physisorption, FTIR, XRD, FESEM, and TEM and evaluated in the reduction of nitrobenzene (NB) to aniline (AN) in a batch process at ambient conditions. The Pd/CSNH shows the highest conversion. Response surface methodology (RSM) was used for investigation of the effect of different variables. The results showed that the mole ratio of sodium borohydride to nitrobenzene has the most important impact on the conversion of nitrobenzene to aniline. In the optimal reaction conditions (20 mg Pd/CSNH and mole ratio of NaBH₄/NB = 4 in 25 min), conversion, selectivity to aniline and yield of 100% were obtained at room temperature.

ARTICLE HISTORY

Received 8 April 2020
Accepted 21 June 2020

KEYWORDS

Nanohybrid material; palladium nanoparticles; spent bleaching earth; nitrobenzene reduction; aniline

Introduction

The extended applications of nitrobenzene (NB) in different industry such as herbicides, insecticides, explosives, pharmaceuticals, and dyes causes to release it in water and soils. But, nitrobenzene is not biodegradable, thus it is extremely toxic for humans according to the United States Environmental Protection Agency (US EPA).^[1,2]

In the last decades, various methods have been studied for degrading NB in water, such as photocatalytic degradation,^[3] chemical oxidation,^[4] ultrasound degradation,^[5] and chemical reduction methods.^[1,2] Since aniline undergoes biodegradation at nature more easily, the chemical reduction method is more capable for treatment of NB polluted water.^[2] In addition, the commercial aniline (AN), produced mainly by catalytic hydrogenation of NB, which is a valuable intermediate for producing of agricultural goods, dyes, pharmaceuticals, and some polymers such as polyurethanes.^[1,2,6]

Among the several reducing agents for effective reduction of nitrobenzene to aniline, one favorable approach is the catalytic reduction in the presence of sodium borohydride in the presence of catalyst.^[7,8]

Up to now, the role of metal nanoparticles as catalyst in this reaction has been extensively studied.^[1,9,10] The Pd and Ni nanoparticles are mostly used for the reduction of nitro compound reactions because of their excellent properties, such as high activity and strong interactions with

hydrogen.^[9–11] However, the stability of nanoparticles is the major problem and it is crucial to design cost-effective support materials that overcome to the aggregation and leaching of nanoparticles.^[2] Therefore, exploring new strategies to manufacturing effective supported metal catalysts with an easy preparation technique is also of great interest.^[12]

Pd nanocatalysts supported on alumina, activated carbon and carbon nanotubes, montmorillonite, SiO₂, MCM-41 meso-materials are reported as effective catalysts in liquid-phase hydrogenation of nitrobenzene under mild conditions.^[2,13–16] The main role of the carbon materials is to disperse and stabilize metal nanoparticles to provide more accessible catalytically active sites compared with bulk metals.^[14] El-Hout et al.^[2] showed a 100% conversion of NB on Pd supported on reduced graphene oxide at room temperature for 3 h. The reduction of NB over magnetically Ni/Graphene nanocomposite using NaBH₄ as reducer in ethanol was examined by Pahalagedara et al.^[15] and 100% conversion at room temperature in 2 h was achieved. Also, Qu et al.^[16] reported 99.9% NB conversion on Pd promoted Ni supported on C₆₀ derivative for 50 min, under 85 °C. They obtained this result using ethanol as solvent and H₂ gas as reducer.

Heterogeneous catalysts based on carbon nanostructures are usually limited to the reduction reaction with organic solvent such as ethanol. In addition, the synthesis of carbon nanostructures with expensive reagents, time consuming

procedure and tedious workup leads to increased catalyst production costs, and the use of hybrid materials can be a solution to decrease this problem.

Clay with a silicate layer structure and eco-friendly nature is a suitable catalyst support with good properties like mechanical and thermal stability, high surface area, and strong metal support interaction. Using carbon/clay hybrid as catalysts may lead to new composite materials with superior activity and better physicochemical properties such as higher hydrophilicity, which help to better dispersion of catalysts in water solvent-based reaction, stronger mechanical properties, low cost, and simplicity in workup. In this sense, carbon/silicate hybrid matrix encapsulated palladium and nickel nanoparticles seem to be useful for reduction of nitrobenzene to aniline.

Spent bleaching earth (SBE) is a useless oil refinery waste material containing a remarkable percentage of remaining oil. Pretreatment of crude oil during a refining process involves degumming, neutralization, bleaching, and deodorization and produces abundant SBE.^[17,18] Bleaching earth is used in this process to absorb the impurity of edible oil. The main component of bleaching earth is SiO₂ because basic elements such as Al leached during the washing the montmorillonite clay with mineral acids. It is expected that about 600,000 metric tons of bleaching earth was applied in the whole world production of oils.^[17,19] The SBE obtained is commonly disposed to landfill with no pretreatment. It can act as a fire hazard (i.e., spontaneous combustion), because it contains 20–40 wt.% of oil which could not be removed by filter pressing.^[20] Because of this much oil, the cement industry has significant difficulty to achieve the high cement quality. On the other hand, burning or landfill disposal will probably become impossible because of environmental restrictions, environmental pollution due to remove of released waste oil, and greenhouse effects.^[19] Therefore, from the environmental, safe, and regulatory points of view, it is urgent to restrict this landfill practice in the future. Recently, the reconsumption of SBE waste to other raw materials has amplified.^[21] The SBE has been used as catalyst material, although a previous extraction of the oil was carried out in these studies.^[22] Therefore, the presence of carbon and silica in the SBE composition could lead to potential smart materials for application in catalytic reactions as catalysts or catalyst supports.

In this work, we report the use of the industrial SBE waste to obtain carbon/silicate nanohybrid material (CSNH) to be used as catalyst support for the selective catalytic reduction of nitrobenzene as toxic substance to a useable and biodegradable product, aniline. Certainly, using waste materials to generate the catalyst make the system more affordable and environmentally friendly.^[19] To maximize the catalytic performance and reusability of the catalyst, the present work also investigates the influence of supported Pd, Ni and Ni-Pd nanoparticles on the reduction reaction under mild operating conditions. For this purpose, the effect of three main factors on the aniline production with effective catalyst, including the amount of the selected catalyst, the mole ratio of NaBH₄ to nitrobenzene and stream time was

studied using response surface methodology (RSM). A central composite design (CCD) was selected for identification of the possible interaction between the factors.

Experimental

Chemicals

The spent bleaching earth (SBE) was obtained from an edible oil refinery plant (Oila Company in Alborz province, Iran). All laboratory chemicals, including ZnCl₂, H₂SO₄, Pd (II) acetate, acetone, Ni(NO₃)₂·6H₂O, nitrobenzene, NaBH₄ were supplied from Merck (Germany) as analytical grade.

Preparation of catalysts

Preparation of carbon/silicate nanohybrid material (CSNH)

To impregnate the SBE with ZnCl₂ (Merck), 100 g of the dried SBE and 45 g of ZnCl₂ were stirred in 250 mL of deionized water using magnetic stirrer, and then heated at about 70 °C in a boiler-reflux condenser for 1 h. Then, impregnated SBE was filtered in a vacuum flask and dried at 105 °C for 24 h.^[23]

Approximately 1.2 g of SBE in a glass tube was placed at the center of the hot zone of the tubular furnace (ribbon Pt-filament). Then, the sample was heated at 150 °C for 30 min under N₂ flow. Subsequently, the temperature was increased at 10 °C min⁻¹ to 450 °C and held for 2 h to make sure the sample was fully pyrolyzed. After that the sample was cooled to below 100 °C under N₂ flow. The resulting product was then washed with 250 mL of 0.5 M of H₂SO₄ (Merck) with a continuous stirring for 3 h. The mixture was filtered and washed with warm deionized water for five times to remove the residues (this sample was named as carbon/silicate nanohybrid material (CSNH)).

Metals loading on the CSNH

The catalysts were prepared by the wet-impregnation method. Typically, CSNH (1 g) was sonicated in 100 mL of deionized water for 15 min, and followed by stirring for 1 h. Then, a certain amount of Pd (II) acetate (Merck) was dissolved in acetone and added dropwise to the CSNH dispersion. The mixture was stirred for 1 h and kept overnight in 70–80 °C to form the catalyst precursor. The catalyst precursor was dried in an oven at 110 °C for 12 h and calcined in a furnace at 500 °C. The catalyst was labeled as Pd/CSNH. Pd-Ni/CSNH and Ni/CSNH catalysts were also prepared in the same procedure using Ni(NO₃)₂·6H₂O (Merck) solution as nickel precursor. The metal content in all three catalysts was 3% of total weight (3 wt.%) and the Pd to Ni weight ratio in Pd-Ni catalyst was 1:1.

Reduction of nitrobenzene to aniline

The catalytic reduction of nitrobenzene was carried out in a standard Pyrex reactor. In a typical reaction, 10 mg of each catalyst was dispersed in 50 mL of nitrobenzene solution (0.123 g/L) in the reactor. Then, 2 mL of fresh aqueous

solution of NaBH_4 (3.8 g/L) was added dropwise to the reactor with a continuous stirring at room temperature. After completing the reaction, 11 mL of the sample was withdrawn and centrifuged prior to analyze it. (The UV-visible spectroscopy was recorded at ordinary time intervals to screen the progress of the reaction).

Conversion of nitrobenzene is calculated as (Equation (1))

$$\% \text{Conversion} = \frac{C_{\text{NB}_0} - C_{\text{NB}_1}}{C_{\text{NB}_0}} \times 100 \quad (1)$$

Where C_{NB_0} is the initial molar concentration of nitrobenzene at the beginning of the reaction and C_{NB_1} is the final molar concentration of nitrobenzene at the end of the reaction.

Characterization of catalysts

Fourier transform infrared (FTIR) spectra were recorded with FTIR spectrometer (a Bruker-VECTOR 33) to make

sure unsaturated oil removal in the SBE. To illustrate the lack of structural change of SBE after thermochemical regeneration and metal loading, the X-ray diffraction (XRD) patterns of the samples were measured with a Bruker D8ADVANCE X-Ray Diffractometer, operating with Ni filtered $\text{Cu-K}\alpha$ radiation (40 kV; 30 mA). Transmission electron microscopy (TEM) (CM-120 Philips) and field emission scanning electron microscopy (FE-SEM) (TESCAN) were used to determine the size and morphology of the samples. The textural properties such as the specific surface area and pore volume were obtained by the standard BET method (BELSORP-mini II, BEL Japan) calculated from pulsed nitrogen adsorption-desorption method at 77 K. The metal content was analyzed by Inductively Coupled Plasma-Mass Spectrometer (ICP-MS), (Perkin-Elmer NexION 300XX). The concentration of NB and its reduction products were analyzed by HPLC (T80⁺ UV/VIS spectrometer, Agilent Technologies Infinity 1260 liquid

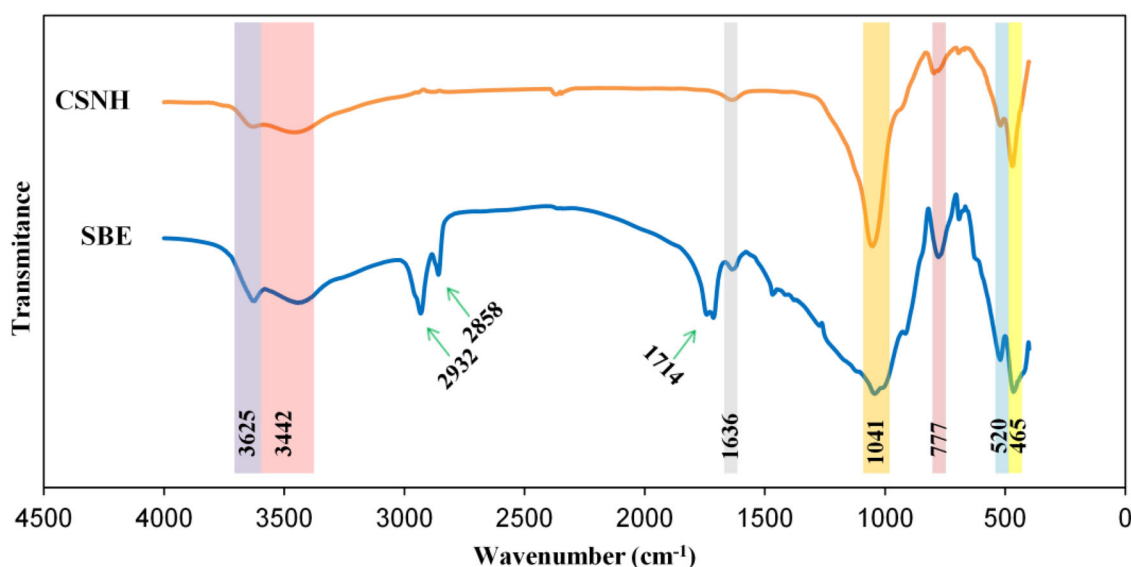


Figure 1. FTIR spectra of SBE and CSNH.

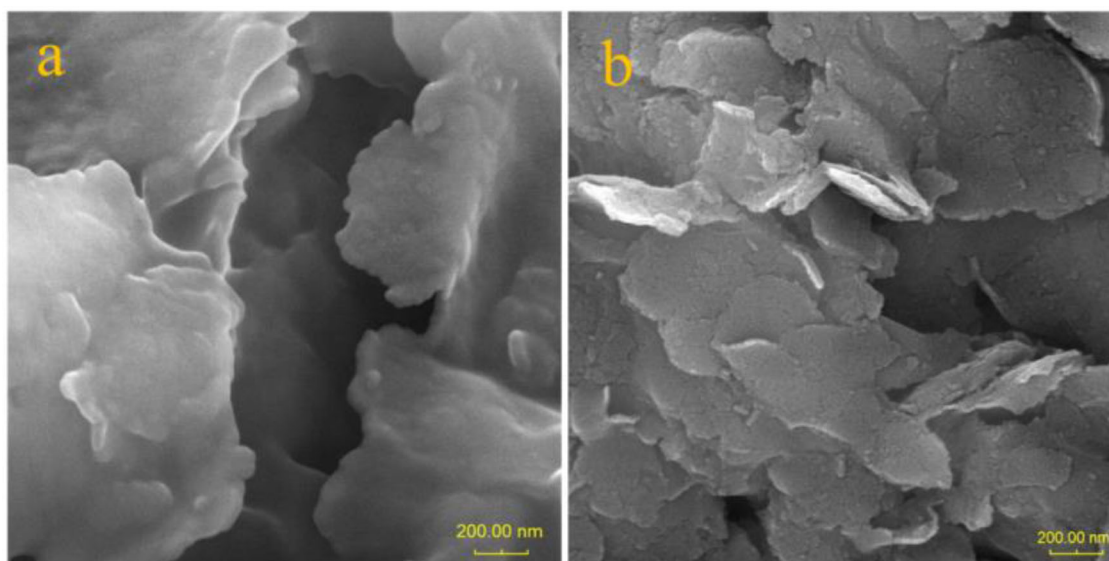


Figure 2. FE-SEM images of (a) SBE and (b) CSNH.

chromatograph with 5 μm (250 \times 4.6 mm) Restek – USA column and methanol/water 65/35 as eluent) to confirm effective catalyst performance in the optimal condition. The recyclability of catalysts was examined by atomic absorption spectrophotometry (AAS) (GBC 932 plus).

Results and discussion

Characterization of the support and catalysts

FTIR spectra of SBE and CSNH are shown in Figure 1. The broad peaks at both samples around 3442 cm^{-1} with a shoulder at 3625 cm^{-1} are attributed to the stretching vibrations of water molecules adsorbed on the silica surface and structural hydroxyls in Si–OH, respectively. The absorption bands of SBE in the region of $2932\text{--}2858\text{ cm}^{-1}$ corresponds to the C–H of carbonaceous chains of oil and the free fatty acids. Also the peak at 1714 cm^{-1} is related to carbonyl vibrations (C=O), which is indicative of the presence of oil in the SBE. These bands disappear in the CSNH sample after pyrolysis treatment. This means that the residual adsorbed organic molecules in the SBE are completely eliminated by the physicochemical treatment.

The absorption bands at 1636 cm^{-1} are indicative of the existence of the interlayer water hydroxyl bending vibration.^[20,24,25] The bands at 1041 cm^{-1} and 777 cm^{-1} are attributed to Si–O stretching vibration.^[20,24,25] Bands at 520 cm^{-1} and 465 cm^{-1} are assigned to bending vibration of Si–O–Al which are the characteristic absorption bands of the montmorillonite.^[24,25] Therefore, the FTIR spectra confirm the presence of the structure of montmorillonite in both materials.

FE-SEM images of the SBE and CSNH are shown in Figure 2. Although both samples exhibit sheet morphology, which is in agreement with the clay mineral structure, it is possible to observe some differences. The thermochemical treatment of SBE provides more plate like particles by removing the residual oil from the surface of parent SBE. The elemental compositions of surface on the catalysts were characterized by EDX analysis. The presence of metal nanoparticles over the CSNH support was confirmed in the EDX detector of SEM (Figure 3 and Table S1).

The crystal structure of the samples was studied using X-ray powder diffraction analysis. Figure 4 shows the XRD patterns of SBE, CSNH, Pd/CSNH, Pd-Ni/CSNH, and Ni/CSNH. As seen in Figure 3 all five samples show the same diffraction pattern which is a characteristic of montmorillonite and silicate structure. Although, the peak intensity of samples are not the same but, clearly, the XRD patterns indicate the physicochemical treatment undergone by SBE and metal loading did not affect on the main structure of parent SBE.^[24–26] This observation is in agreement with the FTIR spectra (Figure 1) and FE-SEM results (Figure 2). However, no diffraction peaks for palladium and nickel was observed in the catalysts due to limited amount of the metals in the samples.

BET method was used to measure the specific surface areas of the support before and after pyrolysis treatment, and the metal catalysts (Table 1). The value of surface area

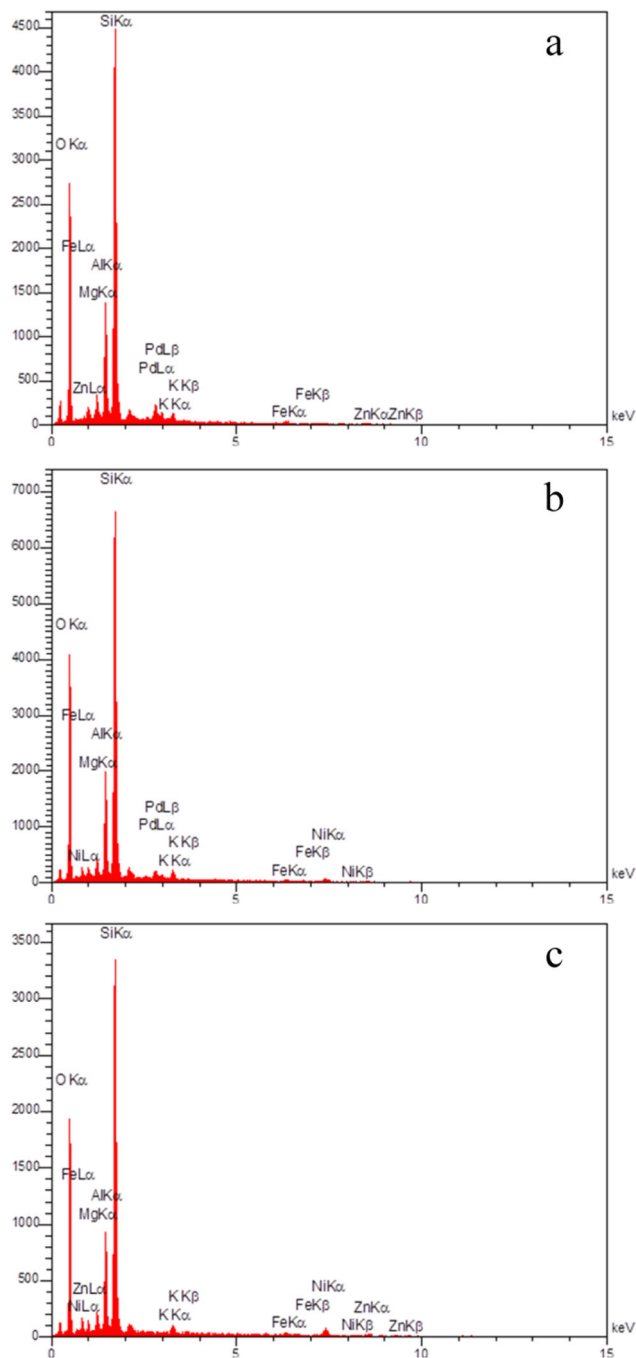


Figure 3. EDX of (a) Pd/CSNH, (b) Pd-Ni/CSNH, and (c) Ni/CSNH.

Table 1. BET surface area.

Sample	Specific surface area (m^2/g)	Pore diameter (nm)	Pore volume (cm^3/g)
SBE	2.5	77.37	0.049
CSNH	14.6	18.8	0.069
Pd/CSNH	102.9	8.4	0.216
Pd-Ni/CSNH	86.4	5.6	0.120
Ni/CSNH	95.3	6	0.143

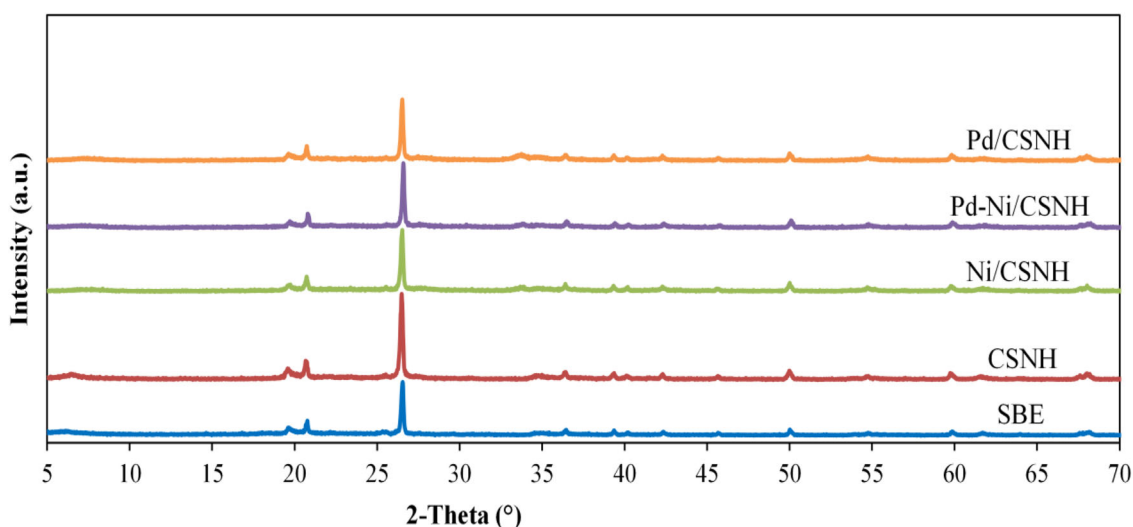


Figure 4. XRD pattern of SBE, CSNH, Ni/CSNH, Pd-Ni/CSNH, and Pd/CSNH.

of SBE increased from 3 to $14.6 \text{ m}^2/\text{g}$ in CSNH due to the first thermochemical treatment but the surface area of catalysts increased impressively by incorporation of metal nanoparticles and second thermal treatment at 500°C . Also, the total pore volumes appeared to increase remarkably from $0.049 \text{ cm}^3/\text{g}$ for SBE to $0.216 \text{ cm}^3/\text{g}$ for Pd/CSNH when the pore diameter decreases around ten times. It seems that the carbonaceous phase of hybrid samples have higher porosity than the parent SBE. As can be seen in Figure S2, the SBE shows an adsorption-desorption isotherm with H3-type hysteresis loop which shows the SBE support has a nonporous structure while the Pd/CSNH catalyst shows an isotherm with H4-type hysteresis loop. Consequently, the thermochemical treatment of SBE and the anchoring of metal nanoparticles onto the CSNH results in an increase of the specific surface area and total pore volume, which is favor for catalytic application.

To study the morphology and size of the Pd/CSNH catalyst, TEM analysis was performed. TEM images of the Pd/CSNH are shown in Figure 5.

The TEM image confirms the Pd nanoparticles have a spherical morphology anchored on the surface of CSNH sheets. This highlighted the advantages of the carbon/silicate nanohybrid material owing to the lattice anchoring effect of metal ions in the layers of CSNH. The HRTEM of the Pd/CSNH catalyst exhibits that the interplanar spacing of the Pd particle is 0.216 nm (consistent with the interplanar distance of the Pd (1 1 1) plane),^[27,28] indicating the Pd particles are in metallic form. PdO_x species were not observed in the sample.

Catalyst activity evaluation

Preliminary test

The UV-visible absorption spectra were recorded for the initial NB solution and treated one in the presence of the only NaBH_4 and CSNH, Ni/CSNH, Pd-Ni/CSNH and Pd/CSNH upon the addition of NaBH_4 (Figure 6). The absorbance peaks at wavelengths of 268 and 235 nm are corresponding to nitrobenzene and aniline, respectively.^[29,30]

As seen in Figure 6, the absorbance peak of NB decreased in the presence of the Pd/CSNH + NaBH_4 which suggests catalytic reduction of nitrobenzene to aniline did not proceed in the absence of catalysts. Also, the yield of aniline decreased in the lack of NaBH_4 , remarkably. The role of CSNH support in the catalytic activity of synthesized catalysts can be related to this fact that carbon species in CSNH structure serve as a medium to accelerate the adsorption of reactants for the reduction of nitrobenzene on the surface of catalysts. Both nitrobenzene and reductant are adsorbed on the surface of carbon species and electrons flow through the carbon to carry out the reaction.^[14]

Totally, the catalysts with palladium showed higher catalytic activity than Ni/CSNH. Because of the specific surface area of Pd-Ni/CSNH ($86.3 \text{ m}^2/\text{g}$) was lower than Ni/CSNH ($95.3 \text{ m}^2/\text{g}$), this order of catalytic activity shows this difference between specific surface of mentioned catalyst could not overcome on the higher catalytic activity of Pd than Ni nanoparticles in the reduction reaction. Although, both mentioned factors have positive synergistic effects on the catalytic activity of Pd/CSNH catalyst in the nitrobenzene reduction reaction. Indeed, the Pd nanoparticles were more active for adsorbing hydrogen molecules than the Ni nanoparticles during reduction of nitrobenzene, due to softer property and a higher electron density. It is clear that the increase in chemisorbed hydrogen atoms on active sites could increase the reduction reaction conversion. In the next step, the chemisorbed hydrogen in the metal-hydrogen bond as nucleophile attack to the nitrogen atom in the nitro group of nitrobenzene and subsequently the nitro group was reduced to the amine group in several steps.^[31,32] However, it is expected the Pd/CSNH with higher surface area and electron density on the active sites, the higher catalytic activity exhibited. Both mentioned factors have positive synergistic effects on the catalytic activity of this catalyst in the nitrobenzene reduction reaction.

It is worth noting that, the Pd-Ni/CSNH catalyst with around 50% palladium content indicates significant reduction conversion. It may be due to the fact that presence of Pd nanocatalyst increases the catalytic activity by formation of a bimetallic structure therefore it can change the electronic states of metals such

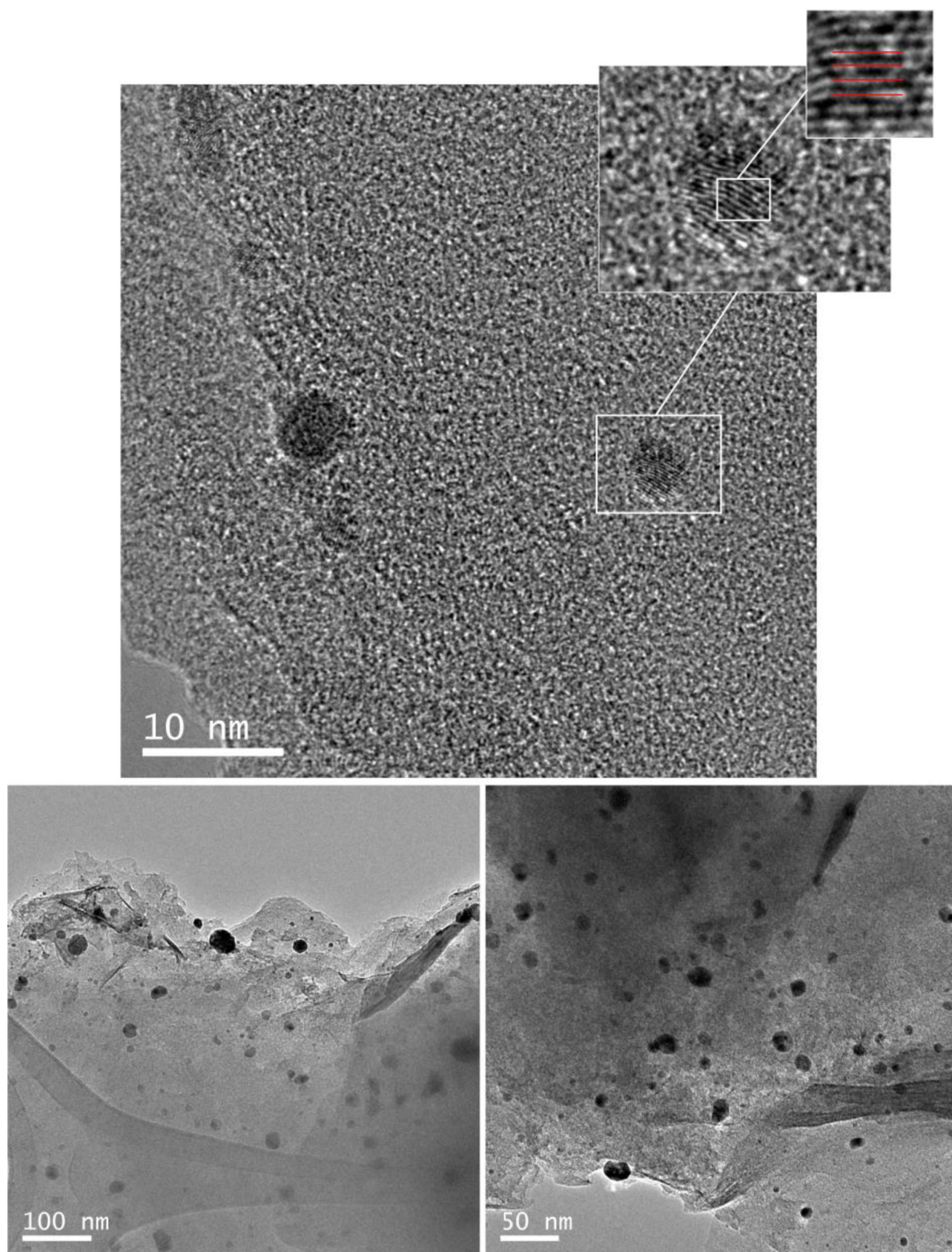


Figure 5. HR-TEM images of Pd/CSNH catalyst.

as their d-band centers. This is in agreement with the catalytic behaviors of Au-Cu alloy and Ni-Pt bimetallic catalyst in reduction of nitro group reported in literature.^[33,34]

Since the efficiency of nitrobenzene reduction for palladium catalyst is higher than other ones, further optimization just done for the Pd catalyst.

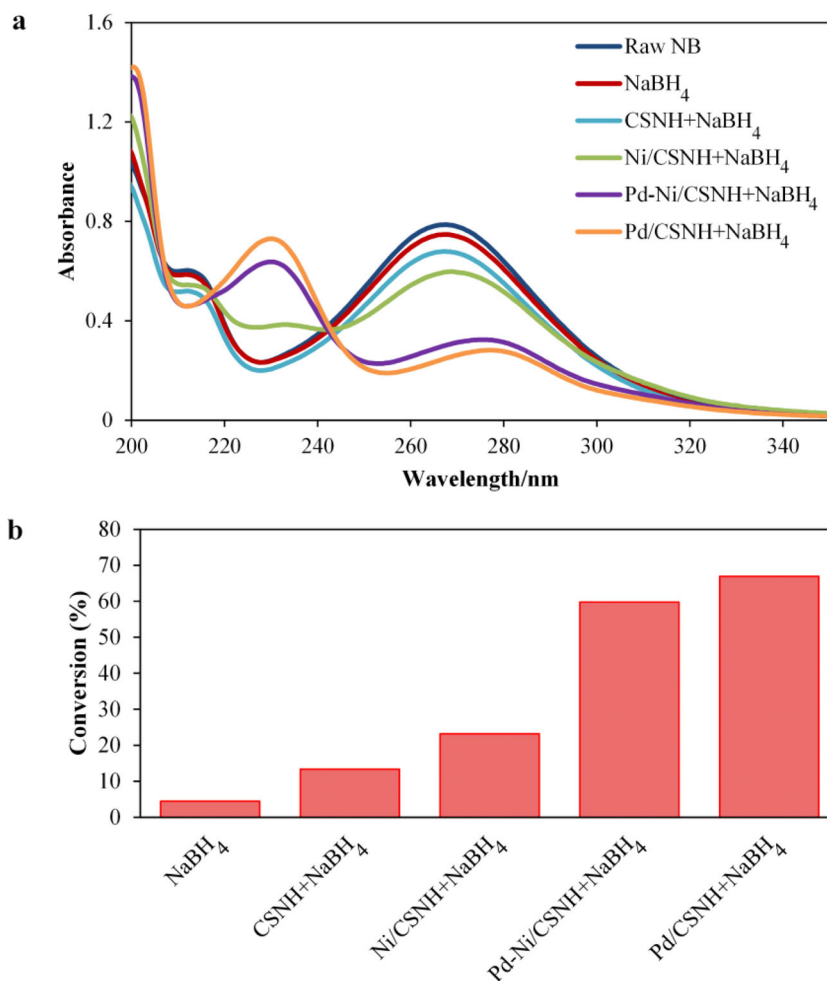


Figure 6. (a) UV spectral change and (b) conversion of nitrobenzene to aniline in the presence of NaBH₄, CSNH + NaBH₄, Ni/CSNH + NaBH₄, Pd-Ni/CSNH + NaBH₄, and Pd/CSNH + NaBH₄.

Process optimization

According to the green chemistry aspects and because of nitrobenzene as a very toxic substance is soluble in the water, it is desired to achieve to the high reaction conversion and aniline yield in the ambient condition (atmospheric pressure and room temperature) and by using water as solvent. So, the nitrobenzene reduction to aniline in the presence of the most effective catalyst in this study (Pd/CSNH) was studied by the central composite design (CCD) with 20 experiment runs. The effect of three factors on catalyst activity, including the weight of catalyst, the mole ratio of NaBH₄/NB and reaction time was investigated. Beside long time experience with these types of chemical reactions, this selection was confirmed as well by a simple statistical analysis performed on the available data. The process parameters involved in the experimental design are demonstrated in Table 2.

In this experimental plan, conversion of nitrobenzene to aniline was selected as response. According to the experimental results, the model (Equation (2)) was predicted for the relationship between conversion and variables.

$$\text{Conversion} = 56.79 - 0.34 \times A + 21.82 \times B + 0.87 \times C \quad (2)$$

where, the A, B, and C parameters are the weight of catalyst, the mole ratio of NaBH₄/NB, and reaction time, respectively.

Table 2. Experimental levels of independent variables.

Variables	Symbol	Variable levels		
		-1	0	1
The weight of catalyst	A	0.0080	0.0125	0.0170
NaBH ₄ /NB	B	1.61	2.5	3.39
Time	C	13.1	25	36.9

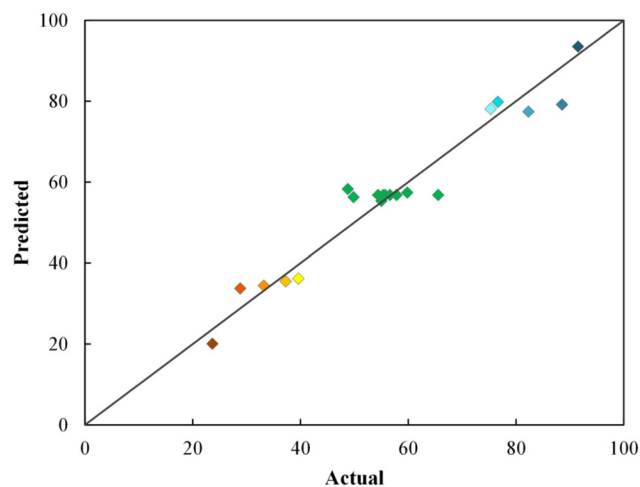


Figure 7. Plot of predicted values vs. actual values for reduction of nitrobenzene using Pd/CSNH catalyst.

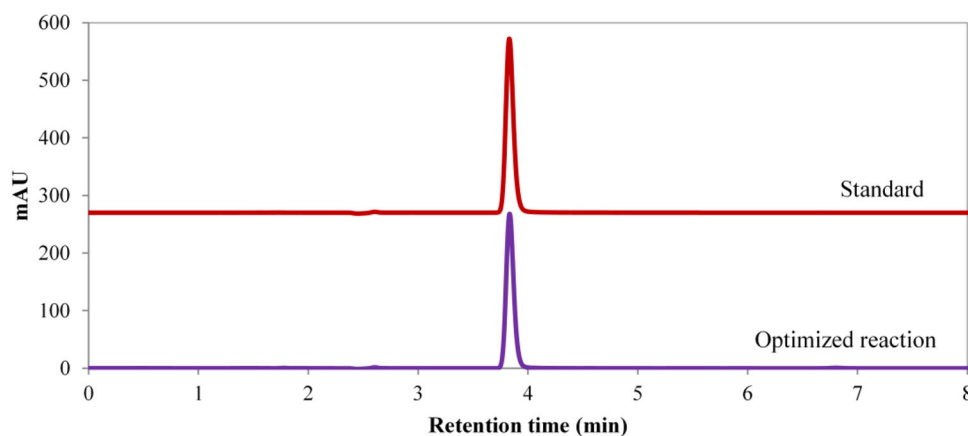


Figure 8. HPLC of reduction of nitrobenzene to aniline in the optimized reaction.

The relations between the process factors and the conversion were studied by analysis of variance (ANOVA). To ensure the statistical statements fit well with the analysis data, the major diagnostic plots (Figures 7 and S3) were used to find out the residual analysis of response surface design. Figure 7 shows the proximity of experimental data and predicted values using the obtained linear model. As depicted in Figure 7, there is superior agreement between predicted and actual values and the plot of residuals versus predicted responses (Figure S3) demonstrated that all points of experimental runs were distributed randomly within the constant range of residuals across the graph, i.e., within the horizontal lines. This result indicates the proposed model is adequate.

According to the results, the most significant factor is the mole ratio of NaBH_4/NB for higher conversion with a statistically significant correlation ($p < 0.0001$) which is in agreement with the previous works.^[35–37] The reduction reaction started by electron transfer from donor borohydride to nitrobenzene as acceptor on the surface of the catalyst and in excess amounts of borohydride the reduction of nitrobenzene to aniline is accomplished quickly. Indeed the concentration of borohydride used as reducing agent must be in excess to remain essentially constant throughout the reaction. For this reason, the kinetic of reduction was more affected by the concentration of sodium borohydride especially at low mole ratio of NaBH_4/NB and the effect of reaction time and the weight of catalyst on the conversion of nitrobenzene in the presence of Pd/CSNH could act well and steadily in the wide range (Figure S4). The best conversion of nitrobenzene was obtained with 20 mg Pd/CSNH and mole ratio of $\text{NaBH}_4/\text{NB} = 4$ in 25 min.

Also, to evaluate final products which are formed under the optimized condition, HPLC analysis was performed (Figure 8).

At the end of the reaction, no peak related to nitrobenzene was detected and only aniline at 3.8 min was found. The result shows the nitrobenzene completely converted to aniline at optimized conditions (Figure 9).

Recyclability and stability of catalyst

The ability to simply separate the catalyst from the reaction mixture and reuse it for next runs is more advantageous of

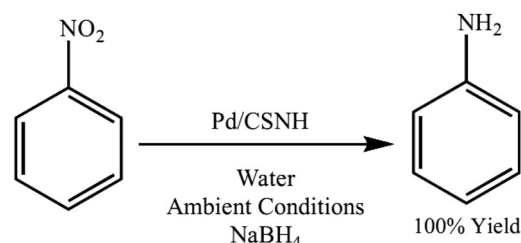


Figure 9. Selective reduction of nitrobenzene to aniline.

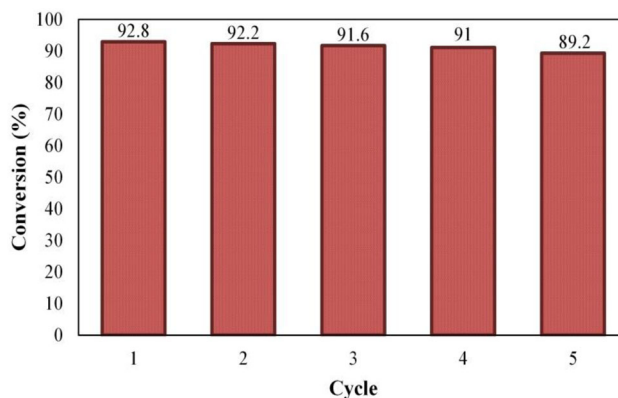


Figure 10. Recycling of Pd/CSNH catalyst.

heterogeneous catalysis than homogenous one. The stability of the Pd/CSNH catalyst was studied at room temperature. The used catalyst was separated by centrifugation from the reaction mixture and then was washed by ethanol solution for the next runs. Figure 10 shows the conversion percentage of the reduction reaction during five cycles. It is observed that the catalyst of Pd/CSNH can be reused at least five runs without significant loss of catalytic activity in the hydrogenation of nitrobenzene to aniline. The maintenance of catalytic activity observed for the recovered Pd/CSNH should originate from the well-stable of the Pd and the active-site isolation, which prevent the Pd nanoparticles aggregation. Catalyst stability was studied with AAS analysis and no Pd content was detected in the solution.

To understand the catalytic efficiency in the NB reduction some literatures are compared and the results are presented in Table 3. In fact, the synthesized nanohybrid in this study is one of the best catalysts with regards to the

Table 3. Comparison of nitrobenzene reduction conversion over various catalysts.

Num.	Catalyst	Reducer	Solvent	Conditions	Conversion	Ref.
1	Pd nanoparticles supported on NH ₂ -UiO-66	formic acid	H ₂ O	60 °C for 7 h	98%	[38]
2	Pd/RGO	NaBH ₄	Ethanol	3 h at room temperature	100%	[2]
3	AuNPs-sPSB	NaBH ₄	Methanol	60 min, 35 °C and N ₂ protective atmosphere (1 bar)	>99%	[39]
4	Ag/ZnO-rGO	Hydrazine	Ethanol	120 min, 80 °C	100	[40]
5	Pd promoted Ni supported on C ₆₀ derivative	H ₂	Ethanol	50 min, 85 °C	>99%	[16]
6	Au-Ag/m-SBA-15	NaBH ₄	Ethanol	120 min, 25 °C	~100%	[41]
7	Pd/meso-γ-Fe ₂ O ₃	H ₂	Ethanol	80 min, 50 °C and 1 atm	~100%	[42]
8	Pd/CSNH	NaBH ₄	Water	25 min at room temperature	100%	In this work

cost effective, eco-friendly and also high nitrobenzene conversion at lower time in the ambient condition.

Conclusions

In this study, the spent bleaching earth as an industrial waste from an edible oil refining factory was converted to the carbon/silicate nanohybrid support for anchoring of palladium and nickel nanoparticles. The catalytic activity of Pd/CSNH, Pd-Ni/CSNH and Ni/CSNH catalysts was investigated toward the reduction reaction of nitrobenzene to aniline by NaBH₄. The preliminary experiment on nitrobenzene reduction was shown the Pd catalyst is the most effective catalyst among all synthesized catalysts due to the higher surface area and electron density on the active sites of the Pd/CSNH. Design of experiment was carried out to study the influence of the variables on the reduction reaction in the presence of Pd catalyst. According to the statistic methodology used in this work, the factor of mole ratio of NaBH₄/NB has the most impact on the reaction conversion at the 95.0% confidence level. At the optimized reaction condition, the catalytic activity of the catalyst was stable for five runs, without any significant decrease in conversion. The present study shows that the Pd/CSNH catalyst is a very promising catalyst for the reduction of nitrobenzene to aniline. Converting the spent bleaching earth, a pollutant of industrial waste to a low cost carbon/silica nanohybrid material offers new and exciting opportunities as a catalyst support for heterogeneous catalysis.

Funding

The authors gratefully acknowledge the financial supports from materials and energy research center (MERC) (Grant No. 771394065) and Spanish National Research Council (iCOOPB20202).

References

- Kim, Y.; Ma, R.; Reddy, D. A.; Kim, T. K. Applied Surface Science Liquid-Phase Pulsed Laser Ablation Synthesis of Graphitized Carbon-Encapsulated Palladium Core – Shell Nanospheres for Catalytic Reduction of Nitrobenzene to Aniline. *Appl. Surf. Sci.* **2015**, *357*, 2112–2120. DOI: 10.1016/j.apsusc.2015.09.193.
- El-Hout, S. I.; El-Sheikh, S. M.; Hassan, H. M. A.; Harraz, F. A.; Ibrahim, I. A.; El-Sharkawy, E. A. A Green Chemical Route for Synthesis of Graphene Supported Palladium Nanoparticles : A Highly Active and Recyclable Catalyst for Reduction of Nitrobenzene. *Appl. Catal. A, Gen.* **2015**, *503*, 176–185. DOI: 10.1016/j.apcata.2015.06.036.
- Jo, W.-K.; Won, Y.; Hwang, I.; Tayade, R. J. Enhanced Photocatalytic Degradation of Aqueous Nitrobenzene Using Graphitic Carbon–TiO₂ Composites. *Ind. Eng. Chem. Res.* **2014**, *53*, 3455–3461. DOI: 10.1021/ie500245d.
- Arslan-Alaton, I.; Ferry, J. L. H₄SiW₁₂O₄₀-Catalyzed Oxidation of Nitrobenzene in Supercritical Water: Kinetic and Mechanistic Aspects. *Appl. Catal. B Environ.* **2002**, *38*, 283–293. DOI: 10.1016/S0926-3373(02)00059-0.
- Xia, K.; Xie, F.; Ma, Y. Degradation of Nitrobenzene in Aqueous Solution by Dual-Pulse Ultrasound Enhanced Electrochemical Process. *Ultrason. Sonochem.* **2014**, *21*, 549–553. DOI: 10.1016/j.ultsonch.2013.09.010.
- Harraz, F. A.; El-Hout, S. E.; Killa, H. M.; Ibrahim, I. A. Palladium Nanoparticles Stabilized by Polyethylene Glycol: Efficient, Recyclable Catalyst for Hydrogenation of Styrene and Nitrobenzene. *J. Catal.* **2012**, *286*, 184–192. DOI: 10.1016/j.jcat.2011.11.001.
- Huang, C.; Hu, J.; Fan, W.; Wu, X.; Qiu, X. Porous Cubic Bismuth Oxide Nanospheres: A Facile Synthesis and Their Conversion to Bismuth during the Reduction of Nitrobenzenes. *Chem. Eng. Sci.* **2015**, *131*, 155–161. DOI: 10.1016/j.ces.2015.03.060.
- Viswanathan, P.; Bhuvaneshwari, T. S.; Ramaraj, R. Investigation on the Catalytic Activity of Aminosilane Stabilized Gold Nanocatalysts towards the Reduction of Nitroaromatics. *Colloids Surf. A* **2017**, *528*, 48–56. DOI: 10.1016/j.colsurfa.2017.05.040.
- Yuan, M.; Yang, R.; Wei, S.; Hu, X.; Xu, D.; Yang, J.; Dong, Z. Ultra-Fine Pd Nanoparticles Confined in a Porous Organic Polymer : A Leaching-and-Aggregation-Resistant Catalyst for the Efficient Reduction of Nitroarenes by NaBH₄. *J. Colloid Interface Sci.* **2019**, *538*, 720–730. DOI: 10.1016/j.jcis.2018.11.065.
- Imura, Y.; Tsujimoto, K.; Morita, C.; Kawai, T. Preparation and Catalytic Activity of Pd and Bimetallic Pd-Ni nanowires. *Langmuir* **2014**, *30*, 5026–5030. DOI: 10.1021/la500811n.
- Qu, Y.; Yang, H.; Wang, S.; Chen, T.; Wang, G. Hydrogenation of Nitrobenzene to Aniline Catalyzed by C60-Stabilized Ni. *Catal. Commun.* **2017**, *97*, 83–87. DOI: 10.1016/j.catcom.2017.04.029.
- Okada, S.; Kamegawa, T.; Mori, K.; Yamashita, H. An Electroless Deposition Technique for the Synthesis of Highly Active and Nano-Sized Pd Particles on Silica Nanosphere. *Catal. Today* **2012**, *185*, 109–112. DOI: 10.1016/j.cattod.2011.08.014.
- Li, L.; Zhang, S.; Lu, B.; Zhu, F.; Cheng, J.; Sun, Z. Nitrobenzene Reduction Using Nanoscale Zero-Valent Iron Supported by Polystyrene Microspheres with Different Surface Functional Groups. *Environ. Sci. Pollut. Res. Int.* **2018**, *25*, 7916–7923. DOI: 10.1007/s11356-017-0854-9.
- Wu, S.; Wen, G.; Zhong, B.; Zhang, B.; Gu, X.; Wang, N.; Su, D. Reduction of Nitrobenzene Catalyzed by Carbon Materials. *Chinese J. Catal.* **2014**, *35*, 914–921. [https://doi.org/10.1016/S1872-2067\(14\)60102-9](https://doi.org/10.1016/S1872-2067(14)60102-9). DOI: 10.1016/S1872-2067(14)60102-9.
- Pahalagedara, M. N.; Pahalagedara, L. R.; He, J.; Miao, R.; Gottlieb, B.; Rathnayake, D.; Suib, S. L. Room Temperature Selective Reduction of Nitrobenzene to Azoxybenzene over Magnetically Separable Urchin-like Ni/Graphene

- Nanocomposites. *J. Catal.* **2016**, 336, 41–48. DOI: [10.1016/j.jcat.2016.01.007](https://doi.org/10.1016/j.jcat.2016.01.007).
16. Qu, Y.; Chen, T.; Wang, G. Hydrogenation of Nitrobenzene Catalyzed by Pd Promoted Ni Supported on C 60 Derivative. *Appl. Surf. Sci.* **2019**, 465, 888–894. DOI: [10.1016/j.apsusc.2018.08.199](https://doi.org/10.1016/j.apsusc.2018.08.199).
 17. Loh, S. K.; James, S.; Ngatiman, M.; Cheong, K. Y.; Choo, Y. M.; Lim, W. S. Enhancement of Palm Oil Refinery Waste–Spent Bleaching Earth (SBE) into Bio Organic Fertilizer and Their Effects on Crop Biomass Growth. *Ind. Crops Prod.* **2013**, 49, 775–781. DOI: [10.1016/j.indcrop.2013.06.016](https://doi.org/10.1016/j.indcrop.2013.06.016).
 18. Lee, S. Y.; Jung, M. Y.; Yoon, S. H. Optimization of the Refining Process of Camellia Seed Oil for Edible Purposes. *Food Sci. Biotechnol.* **2014**, 23, 65–73. DOI: [10.1007/s10068-014-0009-4](https://doi.org/10.1007/s10068-014-0009-4).
 19. Bennett, J. A.; Wilson, K.; Lee, A. F. Catalytic Applications of Waste Derived Materials. *J. Mater. Chem. A* **2016**, 4, 3617–3637. DOI: [10.1039/C5TA09613H](https://doi.org/10.1039/C5TA09613H).
 20. Boey, P. L.; Saleh, M. I.; Sapawe, N.; Ganesan, S.; Maniam, G. P.; Ali, D. M. H. Pyrolysis of Residual Palm Oil in Spent Bleaching Clay by Modified Tubular Furnace and Analysis of the Products by GC-MS. *J. Anal. Appl. Pyrolysis* **2011**, 91, 199–204. DOI: [10.1016/j.jaap.2011.02.010](https://doi.org/10.1016/j.jaap.2011.02.010).
 21. Weng, C. H.; Tsai, C. Z.; Chu, S. H.; Sharma, Y. C. Adsorption Characteristics of Copper(II) onto Spent Activated Clay. *Sep. Purif. Technol.* **2007**, 54, 187–197. DOI: [10.1016/j.seppur.2006.09.009](https://doi.org/10.1016/j.seppur.2006.09.009).
 22. Hindryawati, N.; Daniel, D.; Erwin, E.; Maniam, G. P. Preparation of Spent Bleaching Earth-Supported Calcium from Limestone as Catalyst in Transesterification of Waste Frying Oil. *JBAT*. **2017**, 6, 68–75. DOI: [10.15294/jbat.v6i1.9860](https://doi.org/10.15294/jbat.v6i1.9860).
 23. Tsai, W. T.; Chen, H. P.; Hsien, W. Y.; Lai, C. W.; Lee, M. S. Thermochemical Regeneration of Bleaching Earth Waste with Zinc Chloride. *Resour. Conserv. Recycl.* **2003**, 39, 65–77. [https://doi.org/10.1016/S0921-3449\(02\)00121-0](https://doi.org/10.1016/S0921-3449(02)00121-0). DOI: [10.1016/S0921-3449\(02\)00121-0](https://doi.org/10.1016/S0921-3449(02)00121-0).
 24. Meziti, C.; Boukerroui, A. Regeneration of a Solid Waste from an Edible Oil Refinery. *Ceram. Int.* **2011**, 37, 1953–1957. DOI: [10.1016/j.ceramint.2011.02.016](https://doi.org/10.1016/j.ceramint.2011.02.016).
 25. Mana, M.; Ouali, M.-S. D.; Menorval, L.-C. Removal of Basic Dyes from Aqueous Solutions with a Treated Spent Bleaching Earth. *J. Colloid Interface Sci.* **2007**, 307, 9–16. DOI: [10.1016/j.jcis.2006.11.019](https://doi.org/10.1016/j.jcis.2006.11.019).
 26. Jiang, Y.; Li, X.; Qin, Z.; Ji, H. Preparation of Ni/Bentonite Catalyst and Its Applications in the Catalytic Hydrogenation of Nitrobenzene to Aniline. *Chinese J. Chem. Eng.* **2016**, 24, 1195–1200. DOI: [10.1016/j.cjche.2016.04.030](https://doi.org/10.1016/j.cjche.2016.04.030).
 27. Xiang, Y.; Li, X.; Lu, C.; Ma, L.; Zhang, Q. Water-Improved Heterogeneous Transfer Hydrogenation Using Methanol as Hydrogen Donor over Pd-Based Catalyst. *Appl. Catal. A Gen.* **2010**, 375, 289–294. DOI: [10.1016/j.apcata.2010.01.004](https://doi.org/10.1016/j.apcata.2010.01.004).
 28. Zhang, C.; Cui, X.; Deng, Y.; Shi, F. Active Pd/Fe(OH)_x Catalyst Preparation for Nitrobenzene Hydrogenation by Tracing Aqueous Phase Chlorine Concentrations in the Washing Step of Catalyst Precursors. *Tetrahedron* **2014**, 70, 6050–6054. DOI: [10.1016/j.tet.2014.02.057](https://doi.org/10.1016/j.tet.2014.02.057).
 29. Fu, L.; Cai, W.; Wang, A.; Zheng, Y. Photocatalytic Hydrogenation of Nitrobenzene to Aniline over Tungsten Oxide-Silver Nanowires. *Mater. Lett.* **2015**, 142, 201–203. DOI: [10.1016/j.matlet.2014.12.021](https://doi.org/10.1016/j.matlet.2014.12.021).
 30. Jayabal, S.; Ramaraj, R. Bimetallic Au/Ag Nanorods Embedded in Functionalized Silicate Sol-Gel Matrix as an Efficient Catalyst for Nitrobenzene Reduction. *Appl. Catal. A Gen.* **2014**, 470, 369–375. DOI: [10.1016/j.apcata.2013.10.056](https://doi.org/10.1016/j.apcata.2013.10.056).
 31. Joseph, T.; Vijay Kumar, K.; Ramaswamy, A. V.; Halligudi, S. B. Au-Pt Nanoparticles in Amine Functionalized MCM-41: Catalytic Evaluation in Hydrogenation Reactions. *Catal. Commun.* **2007**, 8, 629–634. DOI: [10.1016/j.catcom.2006.03.004](https://doi.org/10.1016/j.catcom.2006.03.004).
 32. Lin, W.; Cheng, H.; He, L.; Yu, Y.; Zhao, F. High Performance of Ir-Promoted Ni/TiO₂ Catalyst toward the Selective Hydrogenation of Cinnamaldehyde. *J. Catal.* **2013**, 303, 110–116. DOI: [10.1016/j.jcat.2013.03.002](https://doi.org/10.1016/j.jcat.2013.03.002).
 33. Xiao, Q.; Sarina, S.; Waclawik, E. R.; Jia, J.; Chang, J.; Riches, J. D.; Wu, H.; Zheng, Z.; Zhu, H. Alloying Gold with Copper Makes for a Highly Selective Visible-Light Photocatalyst for the Reduction of Nitroaromatics to Anilines. *ACS Catal.* **2016**, 6, 1744–1753. DOI: [10.1021/acscatal.5b02643](https://doi.org/10.1021/acscatal.5b02643).
 34. Shang, H.; Pan, K.; Zhang, L.; Zhang, B.; Xiang, X. Enhanced Activity of Supported Ni Catalysts Promoted by Pt for Rapid Reduction of Aromatic Nitro Compounds. *Nanomaterials* **2016**, 6, 103. DOI: [10.3390/nano6060103](https://doi.org/10.3390/nano6060103).
 35. Bae, S.; Gim, S.; Kim, H.; Hanna, K. Effect of NaBH₄ on Properties of Nanoscale Zero-Valent Iron and Its Catalytic Activity for Reduction of p-Nitrophenol. *Appl. Catal. B Environ.* **2016**, 182, 541–549. DOI: [10.1016/j.apcatb.2015.10.006](https://doi.org/10.1016/j.apcatb.2015.10.006).
 36. Piña, S.; Cedillo, D. M.; Tamez, C.; Izquierdo, N.; Parsons, J. G.; Gutierrez, J. J. Reduction of Nitrobenzene Derivatives Using Sodium Borohydride and Transition Metal Sulfides. *Tetrahedron Lett.* **2014**, 55, 5468–5470. DOI: [10.1016/j.tetlet.2014.08.068](https://doi.org/10.1016/j.tetlet.2014.08.068).
 37. Ajmal, M.; Demirci, S.; Siddiq, M.; Aktas, N.; Sahiner, N. Simultaneous Catalytic Degradation/Reduction of Multiple Organic Compounds by Modifiable p(Methacrylic Acid-Co-Acrylonitrile)-M (M: Cu, Co) Microgel Catalyst Composites. *New J. Chem.* **2016**, 40, 1485–1496. DOI: [10.1039/C5NJ02298C](https://doi.org/10.1039/C5NJ02298C).
 38. Neeli, C. K. P.; Puthiaraj, P.; Lee, Y. R.; Chung, Y. M.; Baeck, S. H.; Ahn, W. S. Transfer Hydrogenation of Nitrobenzene to Aniline in Water Using Pd Nanoparticles Immobilized on Amine-Functionalized UiO-66. *Catal. Today* **2018**, 303, 227–234. DOI: [10.1016/j.cattod.2017.09.002](https://doi.org/10.1016/j.cattod.2017.09.002).
 39. Noschese, A.; Buonerba, A.; Canton, P.; Milione, S.; Capacchione, C.; Grassi, A. Highly Efficient and Selective Reduction of Nitroarenes into Anilines Catalyzed by Gold Nanoparticles Incarcerated in a Nanoporous Polymer Matrix : Role of the Polymeric Support and Insight into the Reaction Mechanism. *J. Catal.* **2016**, 340, 30–40. DOI: [10.1016/j.jcat.2016.05.005](https://doi.org/10.1016/j.jcat.2016.05.005).
 40. Paul, B.; Vadivel, S.; Yadav, N.; Sankar, S. Room Temperature Catalytic Reduction of Nitrobenzene to Azoxybenzene over One Pot Synthesised Reduced Graphene Oxide Decorated with Ag/ZnO Nanocomposite. *Catal. Commun.* **2019**, 124, 71–75. DOI: [10.1016/j.catcom.2019.02.026](https://doi.org/10.1016/j.catcom.2019.02.026).
 41. Sareen, S.; Mutreja, V.; Pal, B.; Singh, S. Synthesis of Bimetallic Au-Ag Alloyed Mesocomposites and Their Catalytic Activity for the Reduction of Nitroaromatics. *Appl. Surf. Sci.* **2018**, 435, 552–562. DOI: [10.1016/j.apsusc.2017.11.152](https://doi.org/10.1016/j.apsusc.2017.11.152).
 42. Jiang, T.; Du, S.; Jafari, T.; Zhong, W.; Sun, Y.; Song, W.; Luo, Z.; Hines, W. A.; Suib, S. L. Synthesis of Mesoporous γ -Fe₂O₃ Supported Palladium Nanoparticles and Investigation of Their Roles as Magnetically Recyclable Catalysts for Nitrobenzene Hydrogenation. *Appl. Catal. A Gen.* **2015**, 502, 105–113. DOI: [10.1016/j.apcata.2015.05.013](https://doi.org/10.1016/j.apcata.2015.05.013).